RECONSTRUCTION-COGNIZANT GRAPH SAMPLING USING GERSHGORIN DISC ALIGNMENT

Yuanchao Bai[*], *Gene Cheung*[†], *Fen Wang*[‡], *Xianming Liu*[$], *Wen Gao*[*]

[*]Peking University, China   [†]York University, Canada
[‡]Xidian University, China   [$]Harbin Institute of Technology, China

ABSTRACT

Graph sampling with noise is a fundamental problem in graph signal processing (GSP). Previous works assume an unbiased least square (LS) signal reconstruction scheme and select samples greedily via expensive extreme eigenvector computation. A popular biased scheme using graph Laplacian regularization (GLR) solves a system of linear equations for its reconstruction. Assuming this GLR-based scheme, we propose a reconstruction-cognizant sampling strategy to maximize the numerical stability of the linear system—*i.e.*, minimize the condition number of the coefficient matrix. Specifically, we maximize the eigenvalue lower bounds of the matrix, represented by left-ends of Gershgorin discs of the coefficient matrix. To accomplish this efficiently, we propose an iterative algorithm to traverse the graph nodes via Breadth First Search (BFS) and align the left-ends of all corresponding Gershgorin discs at lower-bound threshold T using two basic operations: disc shifting and scaling. We then perform binary search to maximize T given a sample budget K. Experiments on real graph data show that the proposed algorithm can effectively promote large eigenvalue lower bounds, and the reconstruction MSE is the same or smaller than existing sampling methods for different budget K at much lower complexity.

Index Terms— Graph sampling, graph Laplacian regularization, Gershgorin circle theorem

1. INTRODUCTION

Graph sampling is a basic problem in *Graph Signal Processing* (GSP) [1–3]. While the noiseless sampling case is extensively studied [4–10], the "sampling with noise" case remains challenging. Previous works typically assume an unbiased *least square* (LS) signal reconstruction scheme from sparse samples [7, 9, 11], which leads to a minimum mean square error (MMSE) formulation and the known A-optimality criterion for independent additive noise [12]. The criterion is minimized greedily per sample using schemes that compute extreme eigenvectors [7, 9], which is not scalable for large graphs. ([11] does not compute eigenvectors, but computes many matrix-vector multiplications for good approximation.)

Instead of unbiased LS reconstruction, recent biased graph signal restoration schemes employ signal priors, including *graph Laplacian regularization* (GLR) [13, 14] and *graph total variation* (GTV) [15–17]. In particular, biased schemes using GLR solve a system of linear equations for signal reconstruction via fast numerical methods like *conjugate gradient* (CG) [18]. In this paper, assuming a GLR signal reconstruction scheme, we propose a *reconstruction-cognizant* sampling strategy to maximize the numerical stability of the linear system—*i.e.*, minimize the condition number (ratio of the largest to smallest eigenvalues) of the coefficient matrix. By coupling the GLR reconstruction method to sampling

during optimization, we expect a better-performing sample set that yields higher quality when the sampling and reconstruction schemes are deployed in tandem.

Computing the extreme eigenvalues of a large matrix directly is expensive, using prevalent methods such as implicitly restarted Arnoldi method [19] or the Krylov-Schur algorithm [20]. Instead, we maximize the minimum of all eigenvalue lower bounds of the matrix, where each bound is represented by the left-end of a Gershgorin disc of the coefficient matrix [21]. We introduce two basic operations to manipulate a Gershgorin disc: disc shifting via sampling, and disc scaling via similarity transform. We design a *Breadth First Iterative Sampling* (BFIS) algorithm to traverse all nodes via *Breath First Search* (BFS), and align the left-ends of all discs to a lower bound threshold T. We then perform binary search (BS) to maximize T given a sampling budget K. *Note that unlike existing greedy sampling schemes [6–9], our scheme never explicitly computes extreme eigenvectors, and thus can scale gracefully to very large graphs.* Experiments on both illustrative examples and real graph data demonstrate that our proposed BS-BFIS algorithm promotes large eigenvalue lower bounds, and the reconstruction MSE is the same or smaller than existing sampling methods [6, 8, 11] for different budget K.

2. PRELIMINARIES

We define a graph $\mathcal{G}$ as a triplet $\mathcal{G}(\mathcal{V}, \mathcal{E}, \mathbf{W})$, where $\mathcal{V}$ and $\mathcal{E}$ represent sets of N nodes and M edges in the graph, respectively. Associated with each edge $(i, j) \in \mathcal{E}$ is a weight $w_{i,j}$, which reflects the correlation or similarity between two nodes i and j. We assume a connected undirected graph; *i.e.*, $w_{i,j} = w_{j,i}, \forall i, j \in \mathcal{V}$. $\mathbf{W}$ is an *adjacency* matrix with $w_{i,j}$ as the (i, j)-th entry of the matrix. Typically, $w_{i,j} > 0$ for $\forall (i, j) \in \mathcal{E}$, and $w_{i,j} = 0$ otherwise.

Given $\mathbf{W}$, the *combinatorial graph Laplacian* matrix Ł is computed as [2]:

$$\text{Ł} \triangleq \mathbf{D} - \mathbf{W} \tag{1}$$

where $\mathbf{D} = \text{diag}(\mathbf{W1})$ is a diagonal *degree* matrix. $\mathbf{1}$ is a vector of all 1's and $\text{diag}(\cdot)$ is an operator that returns a diagonal matrix with the elements of an input vector on the main diagonal.

Graph Laplacian regularizer (GLR) [13] is a smoothness prior for signals on graphs, which has demonstrated its effectiveness in numerous applications, such as semi-supervised learning [22, 23], image processing [3, 13, 14] and computer graphics [24]. Given observation $\mathbf{y}$ on a graph $\mathcal{G}$, one can formulate an optimization for the target signal $\hat{\mathbf{x}} \in \mathbb{R}^N$ using GLR as follows:

$$\hat{\mathbf{x}} = \underset{\mathbf{x}}{\text{argmin}} \|\mathbf{Hx} - \mathbf{y}\|_2^2 + \mu \, \mathbf{x}^\top \text{Ł} \, \mathbf{x} \tag{2}$$

where $\mathbf{H}$ represents a signal degradation process. μ is a tradeoff parameter to balance GLR against the l_2-norm data fidelity term.

In this work, we focus on signal reconstruction from sparse samples. The observation model for signal samples can be modeled linearly as follows [4–11]:

$$\mathbf{y} = \mathbf{H}\mathbf{x} + \mathbf{n} \tag{3}$$

where $\mathbf{H} \in \mathbb{R}^{K \times N}$ is a sampling matrix [11]. $\mathbf{x} \in \mathbb{R}^N$ is an original graph signal, and $\mathbf{y} \in \mathbb{R}^K$, $0 < K < N$, is a sampled signal of dimension K corrupted by additive noise $\mathbf{n}$.

Since objective (2) is quadratic, the optimal solution can be obtained by solving a system of linear equations:

$$(\mathbf{H}^\top \mathbf{H} + \mu \text{\usebox{}})\mathbf{x} = \mathbf{H}^\top \mathbf{y}. \tag{4}$$

Because both $\mathbf{H}^\top \mathbf{H}$ and Ł are singular matrices, (4) can potentially be poorly conditioned. From this observation, we next study the impact of sampling on the numerical stability of (4) and propose a reconstruction-cognizant sampling strategy.

3. RECONSTRUCTION-COGNIZANT SAMPLING

3.1. Graph Sampling and Reconstruction Stability

Reconstructing a sampled signal with GLR leads to solving a linear equation (4). Denote by a diagonal matrix $\mathbf{A} = \mathbf{H}^\top \mathbf{H} \in \mathbb{R}^{N \times N}$ satisfying

$$a_{i,i} = \begin{cases} 1, & i \in \Phi, \\ 0, & \text{otherwise.} \end{cases} \tag{5}$$

where Φ is a set of indices of sampled nodes. Denote by $\mathbf{B} = \mathbf{A} + \mu\text{Ł}$. From *Gershgorin Circle Theorem* (GCT)[1], each eigenvalue λ of $\mathbf{B}$ lies within one *Gershgorin disc* $\Psi_i(b_{i,i}, R_i)$ with disc center $b_{i,i}$ and radius R_i, *i.e.*,

$$b_{i,i} - R_i \leq \lambda \leq b_{i,i} + R_i, \tag{6}$$

where $R_i = \sum_{j \neq i} |b_{i,j}| = \mu \sum_j w_{i,j} = \mu d_i$, and d_i is the degree of node i. The second equation is true since there are no self-loops in $\mathcal{G}$. Center of disc i is $b_{i,i} = \mu d_i + a_{i,i}$.

The upper bound of all eigenvalues can be computed as:

$$\max_i \{ b_{i,i} + R_i \} = \max_i \{ a_{i,i} + 2\mu d_i \} \leq 1 + 2\mu \max_i d_i. \tag{7}$$

For a sparse graph with maximum degree $d_{\max}$ for each node, the eigenvalue upper bound is $1 + 2\mu\, d_{\max}$, which is not large.

The lower bound of all eigenvalues is computed as:

$$\min_i \{ b_{i,i} - R_i \} = \min_i a_{i,i} = 0. \tag{8}$$

In words, for each unsampled node, its Gershgorin disc in $\mathbf{B}$ has left-end at 0—an eigenvalue lower bound at 0. Thus the minimum eigenvalue $\lambda_{\min}$ of $\mathbf{B}$ can also be close to the 0 lower bound, severely magnifying the condition number $\lambda_{\max}/\lambda_{\min}$ of $\mathbf{B}$, and resulting in a poorly-conditioned signal reconstruction using (4). The extreme case is when no nodes are sampled, *i.e.*, $\mathbf{B} = \mu\text{Ł}$, and $\lambda_{\min} = 0$. Ideally then, we would *shift* all Gershgorin discs right to maximize the minimum eigenvalue lower bounds.

Via GCT, we see that we can estimate the degree of numerical instability of GLR signal reconstruction *without* computing actual eigenvalues, by examining left-ends of Gershgorin discs. We next introduce two operations to manipulate Gershgorin discs, which leads to a sampling algorithm to maximize the lower-bounds of $\lambda_{\min}$.

[1]https://en.wikipedia.org/wiki/Gershgorin_circle_theorem

3.2. Graph Sampling to Maximize Lower-bounds of $\lambda_{\min}$

We first state the following linear algebra fact without proof, which we use to enable scaling of Gershgorin discs.

Fact 1: *Similarity transform* $\mathbf{S}$ of a square matrix $\mathbf{B}$ to $\mathbf{C}$, defined as

$$\mathbf{C} = \mathbf{S}\mathbf{B}\mathbf{S}^{-1}, \tag{9}$$

preserves the eigenvalues of $\mathbf{B}$, assuming $\mathbf{S}$ is a nonsingular matrix.

Using Fact 1, we will employ a diagonal $\mathbf{S}$ to scale Gershgorin discs of $\mathbf{B}$, so that left-ends of Gershgorin discs of resulting transformed $\mathbf{C}$ are moved right, maximizing lower bounds of $\lambda_{\min}$. *By scaling each disc Ψ_i to move its left-end $b_{i,i} - R_i$ to the right without affecting eigenvalues of $\mathbf{B}$, we are tightening one lower bound for $\lambda_{\min}$ of $\mathbf{B}$ per scaling operation, which helps us make more informed sampling decisions for other nodes $j \neq i$.*

3.2.1. Breadth First Iterative Sampling

We introduce two basic operations to manipulate Gershgorin discs. The first operation is *disc shifting* via sampling. As discussed, the left-end $b_{i,i} - R_i = a_{i,i}$ of the i-th Gershgorin disc Ψ_i in matrix $\mathbf{B}$ shifts from 0 to 1 when node i is sampled.

The second operation is *disc scaling* via similarity transform. We specify the i-th diagonal term s_i of $\mathbf{S}$ in (9)—and its corresponding element s_i^{-1} in $\mathbf{S}^{-1}$—to scale the radius R_i of Ψ_i and the radii of its neighbors' discs Ψ_j, where $j \in \mathcal{N}_i = \{j \mid w_{i,j} > 0\}$. For example, if we *expand* R_i using scalar $s_i > 1$, then we also *shrink* its neighbors' discs with $s_i^{-1} < 1$. Since s_i is always offset by s_i^{-1} on the main diagonal, the center $b_{i,i}$ of disc Ψ_i is unchanged.

Given graph $\mathcal{G}$ and an eigenvalue lower-bound threshold T, where $T < 1$, we apply disc shifting and scaling operations iteratively to align discs' left-ends at T. The algorithm is as follows. First, we sample a chosen node i (thus moving the corresponding disc Ψ_i's center $b_{i,i}$ from μd_i to $1 + \mu d_i$, and Ψ_i's left-end $a_{i,i}$ from 0 to 1). Then we apply scalar s_i to expand Ψ_i's radius R_i and align its left-end at exactly T. Scalar s_i must hence satisfy

$$a_{i,i} + \mu \left(d_i - s_i \cdot \sum_{j \in \mathcal{N}_i} \frac{w_{i,j}}{s_j} \right) = T, \tag{10}$$

where initially $s_j = 1$ for $j \neq i$. Solving for s_i in (10), we get

$$s_i = \frac{a_{i,i} + \mu\, d_i - T}{\mu \sum_{j \in \mathcal{N}_i} \frac{w_{i,j}}{s_j}}. \tag{11}$$

Using scalar s_i means we also shrink node i's neighbors' discs Ψ_j's radii due to s_i^{-1}. Specifically, left-end $b_{j,j} - R_j$ of a neighbor j's disc Ψ_j ($a_{j,j} = 0$) is now:

$$b_{j,j} - R_j = a_{j,j} + \mu \left(d_j - s_j \cdot \sum_{k \in \mathcal{N}_j \setminus \{i\}} \frac{w_{j,k}}{s_k} - s_j \cdot \frac{w_{j,i}}{s_i} \right) \tag{12}$$

If a neighboring disc Ψ_j's left-end is larger than T, then we need not sample node j and instead expand its radius to align its left-end at T using (11). This shrinks the discs of node j's neighbors, and so on. s_j decreases with hops away from the sampled node.

If the left-end of Ψ_j is smaller than T, then we sample this node ($a_{j,j} = 1$) and select scalar s_j using (11) again, and the process repeats. Since we always expand a current disc ($s_i > 1$) leading to shrinking of neighboring discs ($s_i^{-1} < 1$) in each step, the left-end

Algorithm 1 Breadth First Iterative Sampling

Input: Graph $\mathcal{G}$, lower-bound T, the start node i and μ.
1: Initialize $\mathbf{D} = \text{diag}(\mathbf{W1})$ and $\mathbf{S} = \text{diag}(\mathbf{1})$.
2: Initialize $\mathbf{A} = \text{zeros}(N, N)$, $N = |\mathcal{V}|$.
3: Initialize an empty set $\mathcal{Q}$ for enqueued nodes.
4: Initialize an empty $queue$.
5: $Enqueue(queue, i)$ and $\mathcal{Q} \leftarrow \mathcal{Q} \cup \{i\}$.
6: **while** $queue$ is not empty **do**
7:     $k \leftarrow$ Dequeue($queue$).
8:     Update s_k using (11).
9:     **if** $s_k < 1$ **do**
10:        Sampling node k by setting $a_{k,k} = 1$.
11:        Update s_k using (11).
12:     **endif**
13:     **for** t **in** k's neighbours $\mathcal{N}(k)$ **do**
14:        **if** $t \notin \mathcal{Q}$ **do**
15:           $Enqueue(queue, t)$ and $\mathcal{Q} \leftarrow \mathcal{Q} \cup \{t\}$.
16:        **endif**
17:     **endfor**
18: **endwhile**
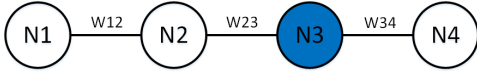**Output:** Sampling matrix $\mathbf{A}$.

Fig. 1: An illustrative example of a 4-node line graph.

of each scaled node remains larger than or equal to lower-bound T. We traverse all the nodes using *Breadth First Search* (BFS). Thus, we name our proposed algorithm *Breadth First Iterative Sampling* (BFIS). The BFIS is sketched in Algorithm 1.

3.2.2. Illustrative Example

We use a simple example to illustrate how BFIS works. We assume a four-node graph as shown in Fig. 1. We start by sampling node 3. Assuming $\mu = 1$, the graph's coefficient matrix $\mathbf{B}$ with $(3, 3)$-th entry updated is shown in Fig. 2a. Correspondingly, left-end of node 3's Gershgorin disc—red dots and blue arrows represent disc centers and radii respectively—shifts from 0 to 1, as shown in Fig. 2d.

    We next perform disc scaling on sampled node 3. As shown in Fig. 2b, scalar s_3 is applied to the third row of $\mathbf{B}$, and thus the radius of disc Ψ_3 is expanded by s_3 where $s_3 > 1$. Simultaneously, scalar s_3^{-1} is applied to the third column, and thus the radii of discs Ψ_2 and Ψ_4 are shrunk due to the scaling of $w_{2,3}$ and $w_{4,3}$ by s_3^{-1}. Note that the $(3, 3)$-th entry of $\mathbf{B}$ (and Ψ_3's disc center) is unchanged, since scalar s_3 is offset by s_3^{-1}. We see that by expanding the disc of sampled node 3, the left-ends of discs of its neighboring nodes (nodes 2 and 4) shift beyond threshold T, as shown in Fig. 2e.

    We next apply scalar s_2 to disc Ψ_2 to expand its radius by s_2, where $s_3 > s_2 > 1$, and the radii of discs Ψ_1 and Ψ_3 are shrunk due to the scaling of $w_{1,2}$ and $w_{3,2}$ by s_2^{-1}, as shown in Fig. 2c. s_2 must be smaller than s_3 for the left-end of Ψ_2 not to move past 0. The discs are shown in Fig. 2f. Subsequently, similar disc operations can be performed on Ψ_1 and Ψ_4. Finally, the left-ends of all discs move beyond threshold T.

3.2.3. Binary Search with BFIS

Given a sample budget K, we perform binary search to maximize the lower-bound threshold T. We call the algorithm *Binary Search with*
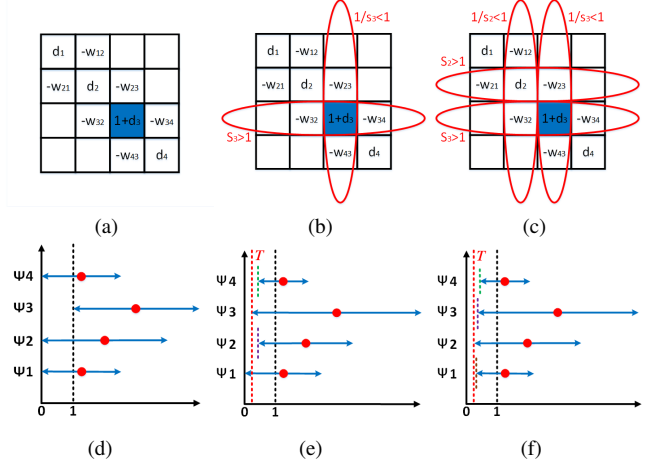

Fig. 2: An illustration of BFIS. (a) sampling node 3. (b) scaling node 3. (c) scaling nodes 2 and 3. (d) Discs after sampling node 3. (e) Discs after scaling node 3. (f) Discs after scaling nodes 2 and 3.

Algorithm 2 Binary Search with BFIS

Input: Graph $\mathcal{G}$, sample size K, numerical precision ϵ, the start node i and weight parameter μ.
1: Initialize $left = 0$, $right = 1$.
2: **while** $right - left > \epsilon$ **do**
3:     $T \leftarrow (left + right)/2$.
4:     $\mathbf{A} \leftarrow \textbf{BFIS}(\mathcal{G}, T, i, \mu)$.
5:     $m \leftarrow$ the number of nodes sampled in $\mathbf{A}$.
6:     **if** $m > K$ **do**
7:        $right \leftarrow T$
8:     **else**
9:        $left \leftarrow T$
10:     **endif**
11: **endwhile**
12: $\hat{T} \leftarrow left$.
13: $\mathbf{A} \leftarrow \textbf{BFIS}(\mathcal{G}, \hat{T}, i)$.
Output: Sampling matrix $\mathbf{A}$, maximum lower-bound $\hat{T}$.

BFIS (BS-BFIS), as outlined in Algorithm 2. At each iteration, if the number of sampled nodes in $\mathbf{A}$ output from BFIS is larger than K, then threshold T is set too large, and we update $right$ to reduce T. On the other hand, if the number of sampled nodes is smaller than or equal to K, then threshold T may be too small, and we update $left$ to increase T. When $right - left \leq \epsilon$, BS-BFIS converges and we find the maximum lower bound $\hat{T}$ with numerical error lower than ϵ. We run BFIS again with $\hat{T}$ to compute the K sampled nodes.

    Because the proposed BFIS executes BFS once on a graph $\mathcal{G}$, the time complexity of BFIS is $O(|\mathcal{V}| + |\mathcal{E}|)$. In order to achieve numerical precision ϵ in BS-BFIS, we need to employ BFIS $O(\log \frac{1}{\epsilon})$ times. Thus, the time complexity for BS-BFIS is $O\left((|\mathcal{V}| + |\mathcal{E}|) \log \frac{1}{\epsilon}\right)$.

4. EXPERIMENTS

4.1. Experimental Setting

We apply the proposed sampling algorithm on both an illustrative line graph and a real *U.S. Climate Normals database* [25]. We compare with several existing graph sampling methods: E-optimal [6],
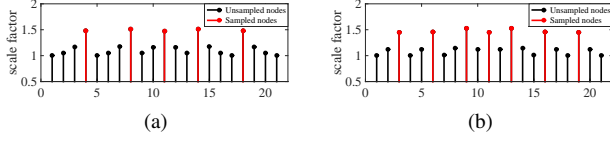
Fig. 3: Sampling on an unweighted line graph, $|\mathcal{V}| = 21$. (a) Sampling 5 nodes, lower-bound $T = 0.048$. (b) Sampling 7 nodes, lower-bound $T = 0.107$.
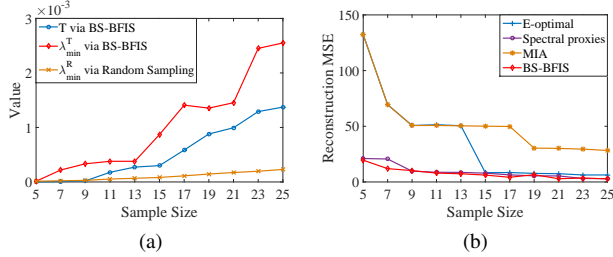

Fig. 4: (a) Comparisons among lower-bound T and the corresponding $\lambda_{\min}^T$ via BS-BFIS, and mean $\lambda_{\min}^R$ via 100 times random sampling. (b) Reconstruction MSE comparisons among E-optimal [6], Spectral proxies [8], MIA [11] and BS-BFIS.

spectral proxies [8], and MIA [11]. All algorithms are implemented and run on Matlab R2015a platform.

To run BS-BFIS algorithm, there are three parameters we need to set besides graph $\mathcal{G}$ and sample size K, *i.e.*, numerical precision ϵ, the start node i and tradeoff parameter μ. In experiments, we set the numerical precision $\epsilon = 10^{-4}$. Because BS-BFIS employs BFS to visit all the graph nodes, the start node i determines the visiting order and affects the performance of BS-BFIS, especially when $K \ll N$. To demonstrate the best performance of BS-BFIS, we choose the start node i that leads to the largest $\hat{T}$ via brute-force search. For the sake of speed, the start node i can be chosen randomly in practice. In experiments, we set the tradeoff parameter μ in (10) and (4) to 0.01 for signal reconstruction.

For experiments on real data, we build a graph on real *U.S. Climate Normals database* [25]. We select 100 temperature stations close to cities with 100 largest populations as graph nodes. The graph edges are connected with *Delaunay Triangulation*[2], and the graph weights are computed using $w_{ij} = \exp(-\|l_i - l_j\|_2^2 / \sigma_l^2) \cdot \exp(-\|\mathbf{x}_i - \mathbf{x}_j\|_2^2 / \sigma_x^2)$ like bilateral filter [26], where l_i and $\mathbf{x}_i$ are the geometric location and the temperature of station i, respectively. $\sigma_l = 5$ and $\sigma_x = 3$. In our experiments, we sample the temperatures of K stations with simulated additive Gaussian noise of unit variance. Then, we reconstruct temperatures of all stations by solving linear equation (4).

4.2. Experimental Results

In Fig. 3, we conduct an illustrative experiment to perform sampling on an unweighted line graph of 21 nodes. We sample 5 and 7 nodes, respectively. Fig. 3a and Fig. 3b report the scale factor s_i for each disc and the distribution of sampled nodes. Using BS-BFIS, we observe periodic uniform sampling for different sampling budgets, which agrees with our intuition.

We also apply BS-BFIS on a graph built on real *U.S. Climate*

---

[2]https://en.wikipedia.org/wiki/Delaunay_triangulation

(a) E-optimal [6]. (b) Spectral proxies [8].

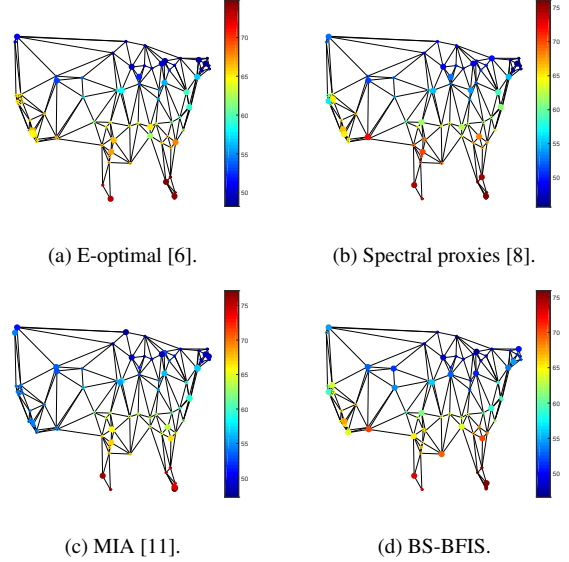(c) MIA [11]. (d) BS-BFIS.

Fig. 5: Sampling visualization ($K = 25$). Solid circles are sampled nodes. Color depicts the temperature. The running time of E-optimal [6], Spectral proxy [8], MIA [11] and BS-BFIS is $0.103s$, $1.440s$, $0.108s$ and $0.082s$, respectively.

Normals database [25]. Our objective is to maximize the lower-bound of minimum eigenvalue $\lambda_{\min}$. We apply BS-BFIS on the constructed graph $\mathcal{G}$ to compute the lower-bound threshold $\hat{T}$ and sampling matrix $\mathbf{A}$ with increasing sample budget K. With output $\mathbf{A}$, we compute $\lambda_{\min}^T$ via eigen-decomposition. For comparison, we employ random sampling 100 times and compute the mean minimum eigenvalue $\lambda_{\min}^R$. As shown in Fig. 4a, BS-BFIS can promote large lower-bound threshold T with increasing sample budget K, and the minimum eigenvalue $\lambda_{\min}^T$ increases correspondingly. Both the lower-bound T and the corresponding $\lambda_{\min}^T$ increases much faster than $\lambda_{\min}^R$ using random sampling.

We also compare the reconstruction MSE of BS-BFIS with existing sampling methods: E-optimal [6], spectral proxies [8], and MIA [11], as shown in Fig. 4b. Each method outputs sampling matrix $\mathbf{A}$ under sampling size K. With $\mathbf{A}$, we can have $\mathbf{H}$ and solve (4) to reconstruct the temperatures of all stations. We observe that the performance of BS-BFIS is comparable to or better than the competing methods. In Fig. 5, we visualize the sampled nodes of the four methods with $K = 25$ and show the running time, respectively. We observe that the sampled nodes of BS-BFIS tend to distribute uniformly on the graph, due to BFS and disc scaling operation in BFIS. However, sampled nodes of other methods, such as MIA [11], tend to accumulate in several areas. This explains the good performance of BS-BFIS. BS-BFIS is the fastest among the four algorithms.

5. CONCLUSION

To address the "graph sampling with noise" problem, in this paper we propose a reconstruction-cognizant graph sampling scheme that assumes a biased reconstruction based on graph Laplacian regularization (GLR) and maximizes the stability of the solution's linear system. In particular, our proposed BS-BFIS promotes large lower-bounds of $\lambda_{\min}$ via Gershgorin disc alignment. Besides stability of signal reconstruction, the proposed algorithm leads to same or better reconstruction MSE against existing methods at lower complexity.

6. REFERENCES

[1] D. I. Shuman, S. K. Narang, P. Frossard, A. Ortega, and P. Vandergheynst, "The emerging field of signal processing on graphs: Extending high-dimensional data analysis to networks and other irregular domains," in *IEEE Signal Processing Magazine*, May 2013, vol. 30, no.3, pp. 83–98.

[2] A. Ortega, P. Frossard, J. Kovacevic, J. M. F. Moura, and P. Vandergheynst, "Graph signal processing: Overview, challenges, and applications," *Proceedings of the IEEE*, vol. 106, no. 5, pp. 808–828, 2018.

[3] G. Cheung, E. Magli, Y. Tanaka, and M. K. Ng, "Graph spectral image processing," *Proceedings of the IEEE*, vol. 106, no. 5, pp. 907–930, 2018.

[4] I. Pesenson, "Sampling in Paley-Wiener spaces on combinatorial graphs," *Transactions of the American Mathematical Society*, vol. 360, no. 10, pp. 5603–5627, 2008.

[5] A. Anis, A. Gadde, and A. Ortega, "Towards a sampling theorem for signals on arbitrary graphs," in *2014 IEEE International Conference on Acoustics, Speech and Signal Processing (ICASSP)*, 2014, pp. 3864–3868.

[6] S. Chen, R. Varma, A. Sandryhaila, and J. Kovačević, "Discrete signal processing on graphs: Sampling theory," *IEEE Transactions on Signal Processing*, vol. 63, no. 24, pp. 6510–6523, 2015.

[7] M. Tsitsvero, S. Barbarossa, and P. Di Lorenzo, "Signals on graphs: Uncertainty principle and sampling," *IEEE Transactions on Signal Processing*, vol. 64, no. 18, pp. 4845–4860, Sep. 2016.

[8] A. Anis, A. Gadde, and A. Ortega, "Efficient sampling set selection for bandlimited graph signals using graph spectral proxies," *IEEE Transactions on Signal Processing*, vol. 64, no. 14, pp. 3775–3789, 2016.

[9] L.F.O Chamon and A. Ribeiro, "Greedy sampling of graph signals," *IEEE Transactions on Signal Processing*, vol. 66, no. 1, pp. 34–47, 2018.

[10] G. Puy, N. Tremblay, R. Gribonval, and P. Vandergheynst, "Random sampling of bandlimited signals on graphs," *Applied and Computational Harmonic Analysis*, vol. 44, no. 2, pp. 446–475, 2018.

[11] F. Wang, Y. Wang, and G. Cheung, "A-optimal sampling and robust reconstruction for graph signals via truncated neumann series," *IEEE Signal Processing Letters*, vol. 25, no. 5, pp. 680–684, 2018.

[12] S. Boyd and L. Vandenberghe, *Convex optimization*, Cambridge University Press, 2004.

[13] J. Pang and G. Cheung, "Graph Laplacian regularization for image denoising: Analysis in the continuous domain," *IEEE Transactions on Image Processing*, vol. 26, no. 4, pp. 1770–1785, April 2017.

[14] X. Liu, G. Cheung, X. Wu, and D. Zhao, "Random walk graph Laplacian based smoothness prior for soft decoding of JPEG images," *IEEE Transactions on Image Processing*, vol. 26, no. 2, pp. 509–524, February 2017.

[15] C. Couprie, L. Grady, L. Najman, J.-C. Pesquet, and H. Talbot, "Dual constrained TV-based regularization on graphs," *SIAM Journal on Imaging Sciences*, vol. 6, no. 3, pp. 1246–1273, 2013.

[16] P. Berger, G. Hannak, and G. Matz, "Graph signal recovery via primal-dual algorithms for total variation minimization," *IEEE Journal of Selected Topics in Signal Processing*, vol. 11, no. 6, pp. 842–855, Sept 2017.

[17] Y. Bai, G. Cheung, X. Liu, and W. Gao, "Graph-based blind image deblurring from a single photograph," *IEEE Transactions on Image Processing*, vol. 28, no. 3, pp. 1404–1418, March 2019.

[18] Magnus Rudolph Hestenes and Eduard Stiefel, *Methods of conjugate gradients for solving linear systems*, vol. 49, Journal of Research of the National Bureau of Standards, 1952.

[19] R. Lehoucq, D. Sorensen, and C. Yang, *ARPACK Users' Guide: Solution of Large-Scale Eigenvalue Problems with Implicitly Restarted Arnoldi Methods*, Society for Industrial and Applied Mathematics, 1998.

[20] G. W. Stewart, "A Krylov–Schur algorithm for large eigenproblems," *SIAM Journal on Matrix Analysis and Applications*, vol. 23, no. 3, pp. 601–614, 2002.

[21] G. Williams, *Linear algebra with applications*, Jones & Bartlett Learning, 2017.

[22] M. Belkin, I. Matveeva, and P. Niyogi, "Regularization and semi-supervised learning on large graphs," in *Learning Theory*, John Shawe-Taylor and Yoram Singer, Eds. 2004, pp. 624–638, Springer Berlin Heidelberg.

[23] G. Cheung, Su W.-T., Mao Y., and Lin C.-W., "Robust semisupervised graph classifier learning with negative edge weights," *IEEE Transactions on Signal and Information Processing over Networks*, vol. 4, no. 4, pp. 712–726, 2018.

[24] O. Sorkine, "Laplacian mesh processing," in *Eurographics 2005 - State of the Art Reports*, Yiorgos Chrysanthou and Marcus Magnor, Eds. 2005, The Eurographics Association.

[25] U.S. Climate Normals Database from National Centers for Environmental Information, "https://www.ncdc.noaa.gov/data-access/land-based-station-data/land-based-datasets/climate-normals/1981-2010-normals-data," .

[26] C. Tomasi and R. Manduchi, "Bilateral filtering for gray and color images," in *Proceedings of the IEEE International Conference on Computer Vision*, Bombay, India, 1998.